Kidney Histopathology and Prediction of Kidney Failure: A Retrospective Cohort Study

Michael T. Eadon[1], **Tae-Hwi Schwantes-An**[2], **Carrie L. Phillips**[3], **Anna R. Roberts**[4], **Colin V. Greene**[1], **Ayman Hallab**[1], **Kyle J. Hart**[1], **Sarah N. Lipp**[1], **Claudio Perez-Ledezma**[1], **Khawaja O. Omar**[1], **Katherine J. Kelly**[1,5], **Sharon M. Moe**[1,5], **Pierre C. Dagher**[1,5], **Tarek M. El-Achkar**[1,5], **Ranjani N. Moorthi**[1]

[1]Division of Nephrology, Indiana University School of Medicine, Indianapolis, IN 46202

[2]Department of Medical and Molecular Genetics, Indiana University School of Medicine, Indianapolis, IN 46202

[3]Department of Pathology, Indiana University School of Medicine, Indianapolis, IN 46202

[4]Regenstrief Institute; Indiana University School of Medicine, Indianapolis, IN 46202

[5]Roudebush Veterans Administration Medical Center, Indianapolis, IN

Abstract

Rationale and Objective—The use of kidney histopathology for predicting kidney failure is not established. We hypothesized that use of histopathological features of kidney biopsy specimens would improve prediction of clinical outcomes made using demographic and clinical variables alone.

Study Design—Retrospective cohort study and development of a clinical prediction model.

Setting and Participants—All 2720 individuals from the Biopsy Biobank Cohort of Indiana who underwent a kidney biopsy between 2002 and 2015 and had at least two years of follow-up.

New Predictors & Established Predictors—Demographic variables, comorbidities, baseline clinical characteristics, and histopathological features.

Outcomes—Time to kidney failure, defined as sustained estimated glomerular filtration rate <= 10 ml/min/1.73 m2.

Analytical Approach—Multivariable Cox regression model with internal validation by bootstrapping. Models including clinical and demographic variables were fit with the addition of histopathological features. To assess the impact of adding a histopathology variable, the amount of variance explained (r^2) and the c-index were calculated. The impact on prediction was assessed by calculating the net reclassification index (NRI) for each histopathological variable and for all combined.

Results—The median follow-up was 3.1 years. Within 5 years of biopsy, 411 patients developed kidney failure (15.1%). Multivariable analyses including demographic and clinical variables revealed that severe glomerular obsolescence (adjusted HR, 2.03; 95% CI, 1.51–2.03), severe interstitial fibrosis and tubular atrophy (IFTA; adjusted HR, 1.99; 95% CI, 1.52–2.59), and severe arteriolar hyalinosis (adjusted HR, 1.53; 95% CI, 1.14–2.05) were independently associated with the primary outcome. The addition of all histopathological variables to the clinical model yielded a net reclassification index for kidney failure of 5.1% (p < 0.001) with a full model c-statistic of 0.915. Analyses addressing the competing risk of death, optimism, or shrinkage did not significantly change the results.

Limitations—Selection bias from use of clinically indicated biopsies and exclusion of patients with less than 2 years of follow-up, as well as reliance on surrogate indicators of kidney failure onset.

Conclusion—A model incorporating histopathological features from kidney biopsy specimens improved prediction of kidney failure and may be valuable clinically. Future studies will be needed to understand if even more detailed characterization of kidney tissue may further improve prognostication about the future trajectory of eGFR.

Introduction

In clinical practice, nephrologists use their experience to estimate the risk of progression to kidney failure. Models employing demographic and laboratory parameters that predict clinical outcomes have been developed in stage 3 chronic kidney disease (CKD) and beyond[1, 2]. Worldwide, the population-standardized annual kidney biopsy rate continues to increase[3]. This rising frequency of biopsies is not unexpected given the importance and accessibility of histopathological interpretation[4, 5]. A challenge for the practicing nephrologist is to integrate renal histopathologic results into their decision-making strategy.

The pathologic evaluation of a kidney biopsy specimen has proven invaluable in determining diagnoses and treatment goals since the 1950s[6, 7]. However, clinicians are confronted with varied diagnoses spanning tubular diseases, CKD, acute kidney injury (AKI), and glomerular diseases. To aid in prognostication across a variety of kidney diseases, it is

important to understand the independent contribution of individual histologic features to kidney disease outcomes.

The integration of histopathology into epidemiologic risk stratification is of active interest. Researchers have reported the prevalence and distribution of various diseases in biopsy cohorts[8–10]. These efforts include the assessment of the correlation of histopathologic findings with outcomes in diabetic nephropathy[11–13] and integration of the MEST criteria in IgA nephropathy prognostication[14, 15]. Further, histopathologic variables were associated with kidney failure outcomes across a spectrum of kidney diseases in a cohort of 676 individuals[16]. We expand upon these findings to analyze outcomes in a large cohort with an extended duration of follow-up across a range of primary diagnoses, including AKI and transplant-related diagnoses, as individuals with these diagnoses will have varying degrees of chronic histopathologic changes as well.

We hypothesize that in those with kidney disease, renal histopathologic features will significantly add to known clinical and demographic predictors of renal survival. The contribution of features like glomerular obsolescence, interstitial fibrosis and tubular atrophy (IFTA), hyaline arteriolosclerosis, nodular mesangial sclerosis, and presence of crescents was assessed in 2720 individuals who underwent biopsy, as well as sub-groups of patients with AKI, CKD, nephritic syndrome, nephrotic syndrome, and transplant-related diagnoses.

Methods

Study Population

This is a clinical prediction model study of all individuals who underwent a kidney biopsy interpreted by Indiana University Health Pathology between 2002 and 2015 with a minimum of 2 years of linked clinical, demographic, and outcome data. These individuals form part of the Biopsy Biobank Cohort of Indiana (BBCI). Individuals meeting inclusion criteria were followed for up to 5 years or until death, kidney failure onset, or the date of last follow-up using electronic health records (EHR). The clinical covariates were obtained retrospectively. The date of first kidney biopsy served as the index date. Of the 5266 individuals with kidney biopsies performed in the Indiana University Health system, complete data (no missing variables) was available for 2720 (Figure S1). This study was approved by the Institutional Review Board at the Indiana University School of Medicine, Indianapolis IN. Due to the retrospective nature of this work, the requirement for informed consent was waived.

Measurements

Demographic and clinical exposure variables—Study cohort data were obtained from the Indiana Network for Patient Care (INPC), a regional Health Information Exchange with data sharing between the five major hospital systems in Indianapolis. Demographic exposure variables included age, self-reported sex, race, and smoking history (never versus ever [past or current]). Comorbidities extracted included coronary artery disease (CAD), congestive heart failure (CHF), diabetes mellitus (DM), and hypertension (HTN), peripheral vascular disease (PVD) as defined by established computer algorithms developed by the Regenstrief Institute[17–19]. These algorithms utilize ICD-9 and ICD-10 codes, clinical

documentation, medication use, and laboratory data to categorize the presence or absence of these conditions in participants.

The estimated glomerular filtration rate (eGFR) at index date and throughout follow-up were determined according to the CKD-EPI creatinine equation[20]. Proteinuria was obtained from the peak 24 hour urine protein collection or spot urinary protein-creatinine ratio within 90 days before or after the index date.

Natural Language Processing—A natural language processing (NLP) program was developed to extract the primary and secondary pathologic diagnoses (Table S1) as well as the five histopathologic variables from the clinical pathology interpretation report in the electronic health record. The pathology reports are templated, increasing success of extraction. The NLP program was iterated until 100% of the diagnoses were captured successfully (F1-score of 1) using manual curation of all biopsy interpretations from the year 2013 as a training set (N = 610). Any diagnoses between 2002 and 2015 that were not recognized by the program were manually checked and the program underwent refinement until all diagnoses were captured. Regarding the five histopathologic exposure variables, one thousand reports were manually reviewed and served as the gold standard. The precision (positive predictive value) of the NLP program was 1.0, the recall (sensitivity) of the program was 0.76. The specificity was 1.0. The F1-score was 0.86. The program flagged variables which were not captured. Of the uncaptured variables across all specimens, 96.3% were able to be obtained upon manual review and 3.7% of uncaptured variables were not recorded in the pathology report. Individuals with any missing variable were excluded.

Histopathologic variables—A single renal pathologist (C.P.) interpreted 95.5% of all specimens. Crescents and nodular mesangial sclerosis were reported as bi-level variables according to their presence or absence. Cellular or fibrocellular crescents were treated as presence of crescents; fibrous crescents (more than 75% fibrous matrix and less than 25% cells and fibrin) alone were treated as absence of crescents[21]. Nodular mesangial sclerosis was considered present if at least one glomerulus had diffuse nodular expansion of the mesangial matrix[22, 23]. Glomerular obsolescence, arteriolar hyalinosis and IFTA were recorded by the pathologist as either the proportion of kidney parenchyma affected (0–100%) or as discrete terms (absent, mild, moderate, or diffuse/widespread). These variables were categorized on a scale from 0–3 with 0 corresponding to absence or 10% of kidney affected; 1, mild or 11%−30% of kidney affected; 2, moderate or 31%−60% of kidney affected; and 3, diffuse or >60% of kidney affected.

Outcome variables—The primary outcome was time to kidney failure, calculated in days from the time of kidney biopsy. Since initiation of dialysis was not consistently differentiated from AKI in the INPC, the kidney failure was defined as 6 months of sustained eGFR 10 ml/min/1.73m^2, using the first date of the sustained eGFR 10 ml/min/1.73m^2. The use of a sustained low eGFR as a surrogate of kidney failure onset allowed excluding AKI from the outcome definition. Death was ascertained from INPC records and the National Death Index database for the competing risk model. The last date of EHR data extraction was 12/31/2017. Right censoring at 5 y (1825 days) from the biopsy was used for all outcomes.

Statistical Analysis

Baseline demographic characteristics, comorbidities, eGFR, and proteinuria at the time of biopsy were summarized and expressed as a percent prevalence for categorical variables and as median and inter-quartile range (IQR) for continuous variables. Univariable cox proportional hazards survival analyses were conducted to explore the relationship between exposure variables and the outcome of interest. Multivariable Cox regression survival analyses tested each outcome to assess the contribution of histopathologic features after adjusting for clinical characteristics. Significant deviations from proportionality assumptions were assessed and adjusted for in the multivariable models. The clinical model for the primary outcome included age, sex, race, CHF, PVD, DM, HTN, CAD, smoking history, baseline eGFR, its interaction with time, and proteinuria as covariates. The time interaction term for eGFR (per 365 days) was included to adjust for a cox proportional hazard assumption violation in the baseline eGFR variable. The hazard associated with baseline eGFR was expressed per 10 ml/min/1.73 m^2. Clinical-pathology models were built, each including all covariates from the clinical model with the addition of one pathological feature of interest: glomerular obsolescence, IFTA, arteriolar hyalinosis, or presence of crescents or nodular mesangial sclerosis. To assess the effect of adding a pathologic variable to each model, we calculated the amount of variance explained (r^2) and c-index. To show improvement in prediction, net reclassification index (NRI) was calculated for each histopathologic variable when added to the full clinical model.

Internal validation was performed by 2,500 bootstrapping runs to determine the degree of optimism in each hazard ratio estimate for each histopathologic variable[24], as well as both parameter-wise and global shrinkage factors to adjust the estimated regression coefficients for overfitting using the dfbeta method. Finally, a model that included all demographic, clinical and histopathological factors with the outcome of interest assessed the improvement in proportion of overall variance explained, c-index, and NRI.

Disease status sub-group tests were conducted for AKI, CKD, nephritic, nephrotic, and transplant-related diagnosis sub-groups. Using a regression model for each histopathologic variable, all demographic variables, clinical variables, primary diagnosis sub-group, and diagnosis interaction terms were fitted to calculate adjusted hazard ratios for each sub-group. Heterogeneity of the effect estimates from different diagnosis sub-groups was assessed by testing the significance of the relevant histologic feature x disease sub-group interaction term. Two-sided p-values of < 0.05 and < 0.001 were denoted in the text. Schoenfelds residuals were assessed for overall models as well as within sub-groups to establish model fit[25].

Sensitivity analyses were performed using cumulative incidence plots to account for competing risks of kidney failure and death. Fine and Gray models were calculated to account for the competing risk of death with kidney failure.

Results

Demographics and Clinical characteristics

In total, 2720 individuals were included in the analysis with complete demographic, clinical, comorbidity, biopsy, and follow-up data for the primary outcome (Table 1). The median age was 43 years; those included were predominantly white (71.8%) and about half were female (49.7%). Clinical diabetes was present in 37.8% and the median eGFR at biopsy was 38.7 (IQR, 20.4–60.5) ml/min/1.73m^2. Median proteinuria was 2.1 (IQR, 0.6–5.9) g/d.

Histopathologic features and diagnoses

The median percentage of obsolescent glomeruli per biopsy was 10% (IQR, 0%−31.5%). Nodular mesangial sclerosis was observed in 9.4% and crescents were found in 13.9% of biopsy specimens. Severe IFTA was noted in 14.4% of biopsy specimens. The majority of biopsy specimens had at least mild arteriolar hyalinosis (56.9%), with 11.5% interpreted as having severe hyalinosis.

Biopsy specimens were categorized according to their primary diagnosis as AKI, CKD, nephritic syndrome, nephrotic syndrome, or a kidney transplant-related diagnosis (Table 2). Nephritic syndrome accounted for 29.7% of primary diagnoses and AKI accounted for only 10.3%.

Primary outcome analysis

In a median follow-up of 1145 days (354–1825), 411 (15.1%) individuals reached the primary outcome of kidney failure. In univariable analysis, statistically significant demographic covariates included age and black race, which increased the hazard ratio for the endpoint (Table 3). A lower baseline eGFR was significantly associated with shorter time to kidney failure. Likewise, higher baseline proteinuria (HR, 1.04; 95% CI, 1.03–1.05) and comorbidities such as CHF, PVD, DM, HTN, CAD, and smoking history all increased the risk of the composite outcome (all $p < 0.05$).

Unadjusted eGFR alone explained 12.9% of the variance in time to kidney failure; however, the effect of baseline eGFR on survival was non-proportional over time. To correct for this, a multivariable analysis of the primary outcome included eGFR and its interaction with time. In the multivariable clinical model, exposure variables including baseline eGFR, proteinuria, black race, CHF, CAD, and smoking history all retained significance for time to kidney failure (all $p < 0.05$). This model explained 32.0% of the variance in time to kidney failure.

The key histopathologic features that were significantly associated with time to kidney failure in the univariable analysis included arteriolar hyalinosis, IFTA, nodule formation, and glomerular obsolescence (Table 4). Unadjusted associations are illustrated in Figure 1 (row 1). Each histopathologic variable was then queried in the multivariable clinical model to determine adjusted significance. Any level of glomerular obsolescence conferred an increased hazard for time to the composite outcome (adjusted HR of 2.03 [95% CI, 1.51–2.74] for severe glomerular obsolescence). Additional histologic features that improved prediction of the primary outcome over the clinical model included the presence of severe

hyaline arteriolosclerosis (adjusted HR, 1.53; 95% CI, 1.14–2.05) and IFTA (HR of 1.99 [95% CI, 1.52–2.59] for diffuse IFTA). The presence of cellular or fibrocellular crescents was associated with decreased progression to the primary outcome in the univariable model, but not the multivariable model. The histopathologic predictors were all moderately correlated (Table S2). When all histopathologic variables were added to construct a fully adjusted clinical-pathology model, the net reclassification index was 5.1% over the clinical model alone (p < 0.001).

Internal validation

To evaluate the prediction model performance, internal validation was performed by bootstrapping with 2500 iterations. The hazard ratio, c-statistic, and net reclassification index for the histopathologic variables are presented in Table S3 after correction for optimism. The model was not optimistic as the c-statistic was 0.91 before and after correction for optimism. Analogously, shrinkage factors were calculated to adjust for overfitting using a penalized maximum likelihood method for parameter-wise factors of shrinkage during estimation and a uniform shrinkage method for adjustment after estimation. The uniform shrinkage factor was 0.96. Adjusted hazard ratios for the significant histopathologic variables changed minimally and are provided in Table S4.

Sensitivity analysis

During follow-up, 256 individuals (9.4%) died. A Fine and Gray sensitivity analysis was employed to assess time to kidney failure with death as a competing risk (Table S5). Significant associations were identified between time to kidney failure with moderate and severe glomerular obsolescence, moderate and severe IFTA, and severe arteriolar hyalinosis. Cumulative incidence plots are depicted in Figure S2.

Disease sub-group analyses

Individuals were categorized into one of five sub-groups based on primary histopathologic diagnoses. Kaplan Meier curves (Figure 1, rows 2–6) illustrate the unadjusted relationships between histopathologic characteristics and outcome-free survival according to disease state sub-group. Distinct histopathological features were associated with time to kidney failure in the disease sub-groups. For example, glomerular obsolescence was associated with the primary outcome in all sub-groups except transplant-related diagnosis (all p < 0.001).

In a multivariable analysis of the 2513 individuals in each of the five sub-groups, the histopathologic variables were added to the fully adjusted clinical model along with diagnosis sub-group variables and interaction terms (Table 5). The 207 individuals without sub-group categorization ("Other" in Table 2) were excluded in the analysis. Significant heterogeneity was identified between disease sub-groups for the following predictors: severe arteriolar hyalinosis, moderate or severe IFTA, and moderate or severe glomerular obsolescence. For AKI, the significant predictors of time to kidney failure were severe arteriolar hyalinosis, IFTA, nodular mesangial sclerosis, and any level of glomerular obsolescence. IFTA and glomerular obsolescence were also significant covariates for nephritic disease. In contrast fewer predictors were significant in the CKD, nephrotic syndrome, and transplant-related diagnosis sub-groups.

Discussion

In this retrospective cohort study, we established that common histopathologic features facilitate improved prediction of kidney failure. After accounting for an adjusted clinical model, three exposure variables added predictive value for kidney failure: arteriolar hyalinosis, IFTA, and glomerular obsolescence. Strong associations were identified; for example, widespread interstitial fibrosis and tubular atrophy increased the hazard for kidney failure by 99%. Similarly, widespread glomerular obsolescence increased hazard of the primary outcome by 103%.

Significant strengths of our analysis included a large cohort with sample size of 2720 individuals with no missing data. Internal validation was performed by bootstrapping, revealing minimal optimism. All individuals were followed for between 2 to 5 years for a clinical outcome of kidney failure. A sensitivity analysis for the competing risk of kidney failure and death did not alter conclusions. Furthermore, the use of a natural language processing algorithm expedited and normalized data collection as compared to a manual review by multiple humans. Due to the sample size and the assignment of primary diagnoses, we examined sub-groups based on categorized disease states, showing heterogeneity between disease categories. The histopathologic features most relevant to outcomes were determined within each sub-group.

We hypothesized that prognostication of kidney failure could be improved by incorporating histopathologic features into a clinical model. The null hypothesis was rejected. When clinical characteristics and histopathologic features were combined, the overall proportion of variance explained by the addition of histopathologic features was improved significantly by 1.0%, yielding a fully adjusted r^2 of 33.0%. The net reclassification rate after including all histopathologic predictors in a fully adjusted model was 5.1%. Even after accounting for the exposure variables queried, the majority of the hazard for kidney failure remains unexplained. Thus, considerable opportunity remains to improve the predictive value of a histologic interpretation by uncovering novel molecular markers to aid the renal pathologist.

Our results expand the current body of literature, but also maintain portability to include within existing model systems of renal risk stratification. Current clinical models allow the determination of kidney disease progression risk. Tangri et. al described kidney failure risk models that were developed across broad cohorts[26]. These include a 4-variable model of age, sex, eGFR, and albuminuria, and a 6 variable model with diabetes and hypertension. Our clinical model included these variables, as well as additional comorbidities such as CHF, CAD, PVD, and smoking. The 5-year follow-up in this analysis matches the risk prediction models. Analogously, the histologic exposure variables align closely with the consensus guidelines of the Renal Pathology Society[27]. This included assignment of a primary diagnosis, itemizing coexisting lesions as secondary diagnoses, and standardized scoring of light microscopic features. There were exceptions to the consensus guidelines; for example, our threshold for widespread or diffuse glomerular obsolescence, IFTA, or arteriolar hyalinosis was 60% rather than 50%, in part because the guidelines were released after our study period ended.

Multiple efforts have tested the association of histopathologic findings with outcomes, including diabetic nephropathy[11–13]. In our cohort, diabetic nephropathy accounted for 8.8% of primary diagnoses. Waikar et. al assessed histopathologic characteristics in a broader cohort of 676 individuals without transplant, identifying glomerular obsolescence, IFTA, arterial sclerosis, and arteriolar sclerosis as predictors of future kidney failure[16]. From these studies, we derived the clinical and histopathologic exposure variables to query. Of the 2720 individuals in our cohort, only about half had a primary diagnosis of nephritic syndrome or nephrotic syndrome and about 20% were transplant biopsies. This supports the generalizability of our results across a spectrum of diagnoses. However, we conducted secondary analyses in disease sub-types to complement the findings of the entire cohort. Some insight might be drawn from these sub-group analyses as the exposure variables held greater significance in AKI and nephritic syndrome than the other disease sub-groups. For example, the significance of IFTA in nephritic syndrome aligns with what Striker et. al described in 1970[28, 29]. The greater significance of histopathologic predictors in AKI and nephritic syndrome is not surprising. Baseline eGFR explains a large proportion of variance in our model and eGFR can change substantially from the time of biopsy during the recovery of AKI or treatment of nephritic disease. Herein, the histopathologic variables of chronicity may hold greater predictive value in these conditions.

Several limitations were identified. These limitations include the presence of selection bias as all biopsies were clinically indicated by a nephrologist. Results must be interpreted cautiously as they may not apply to all patients with CKD, especially those who do not have indications for a kidney biopsy. The requirement for sufficient follow-up may have excluded individuals from the analysis with a good prognosis who did not receive 2 years of follow-up care. Actual dialysis initiation dates were not available for the entire cohort. To overcome this, a surrogate outcome of sustained eGFR <= 10 ml/min/1.73 m2 was employed. In this study, the biopsy specimens were not re-evaluated beyond their surgical pathology consultation and 95.5% of all biopsy specimens were interpreted by a single renal pathologist. Interpretation by a single pathologist may introduce subjectivity or idiosyncratic pathology interpretations that could limit the applicability of results to other centers. Sub-groups were defined by primary diagnoses and categorized according to major disease classifications, which reduced specificity. For example, lupus nephritis can present as thrombotic microangiopathy, nephrotic syndrome, or nephritic syndrome, and may also have secondary acute tubular necrosis. Ultimately, sub-group categorization was based on perceived clinician utility, balancing sample size with specificity and complexity. Finally, the clinical model introduced in this study was internally validated by bootstrapping[24]; external validation in a second cohort is an important future direction.

As immunofluorescence and electron microscopy improve the predictive and diagnostic capability of a renal biopsy interpretation[30], the advancement of molecular characterization and next generation imaging analyses may further augment the value of a kidney biopsy specimen[31–33]. Novel transcriptomic, proteomic, and imaging signatures will allow refinement of disease classification by identifying therapeutic interventions more likely to succeed or improving prognostication of recovery and progression to kidney failure. Several endeavors have succeeded in identifying unique transcriptomic pathways, novel disease markers, and expression quantitative trait loci in kidney biopsy specimens[31, 34–36]. In order

to better understand the independent predictive value of novel markers to kidney disease outcomes, it is important to determine the degree to which established histopathologic features contribute to renal prognosis. This understanding will facilitate an appreciation for the value novel markers that add to the important value of a histopathologic interpretation by a renal pathologist.

Supplementary Material

Refer to Web version on PubMed Central for supplementary material.

Acknowledgements

References

1. Tangri N, Stevens LA, Griffith J, et al. A predictive model for progression of chronic kidney disease to kidney failure. Jama. 2011;305(15): 1553–1559. [PubMed: 21482743]

2. Chronic Kidney Disease Prognosis C. Grams ME, Sang Y, Ballew SH, et al., for the Chronic Kidney Disease Prognosis Consortium. Predicting timing of clinical outcomes in patients with chronic kidney disease and severely decreased glomerular filtration rate. Kidney Int. 2018;93:1442–1451. Kidney Int. 2018;94(5): 1025–1026. [PubMed: 29605094]

3. Cunningham A, Benediktsson H, Muruve DA, Hildebrand AM, Ravani P. Trends in Biopsy-Based Diagnosis of Kidney Disease: A Population Study. Can J Kidney Health Dis. 2018;5: 2054358118799690. [PubMed: 30263130]

4. Covic A, Schiller A, Volovat C, et al. Epidemiology of renal disease in Romania: a 10 year review of two regional renal biopsy databases. Nephrol Dial Transplant. 2006;21(2): 419–424. [PubMed: 16249204]

5. Rychlik I, Jancova E, Tesar V, et al. The Czech registry of renal biopsies. Occurrence of renal diseases in the years 1994–2000. Nephrol Dial Transplant. 2004;19(12): 3040–3049. [PubMed: 15507479]

6. Luciano RL, Moeckel GW. Update on the Native Kidney Biopsy: Core Curriculum 2019. Am J Kidney Dis. 2019;73(3): 404–415. [PubMed: 30661724]

7. Kark RM, Muehrcke RC. Biopsy of kidney in prone position. Lancet. 1954;266(6821): 1047–1049. [PubMed: 13164322]

8. Sim JJ, Batech M, Hever A, et al. Distribution of Biopsy-Proven Presumed Primary Glomerulonephropathies in 2000–2011 Among a Racially and Ethnically Diverse US Population. Am J Kidney Dis. 2016;68(4): 533–544. [PubMed: 27138468]

9. Murugapandian S, Mansour I, Hudeeb M, et al. Epidemiology of Glomerular Disease in Southern Arizona: Review of 10-Year Renal Biopsy Data. Medicine (Baltimore). 2016;95(18): e3633. [PubMed: 27149502]

10. O'Shaughnessy MM, Hogan SL, Thompson BD, Coppo R, Fogo AB, Jennette JC. Glomerular disease frequencies by race, sex and region: results from the International Kidney Biopsy Survey. Nephrol Dial Transplant. 2018;33(4): 661–669. [PubMed: 29106637]

11. Mottl AK, Gasim A, Schober FP, et al. Segmental Sclerosis and Extracapillary Hypercellularity Predict Diabetic ESRD. J Am Soc Nephrol. 2018;29(2): 694–703. [PubMed: 29180393]

12. Nair V, Komorowsky CV, Weil EJ, et al. A molecular morphometric approach to diabetic kidney disease can link structure to function and outcome. Kidney Int. 2018;93(2): 439–449. [PubMed: 29054530]

13. Fufaa GD, Weil EJ, Lemley KV, et al. Structural Predictors of Loss of Renal Function in American Indians with Type 2 Diabetes. Clin J Am Soc Nephrol. 2016;11(2): 254–261. [PubMed: 26792530]

14. Chen T, Li X, Li Y, et al. Prediction and Risk Stratification of Kidney Outcomes in IgA Nephropathy. Am J Kidney Dis. 2019;74(3): 300–309. [PubMed: 31031086]

15. Barbour SJ, Coppo R, Zhang H, et al. Evaluating a New International Risk-Prediction Tool in IgA Nephropathy. JAMA Intern Med. 2019;179(7): 942–952. [PubMed: 30980653]

16. Srivastava A, Palsson R, Kaze AD, et al. The Prognostic Value of Histopathologic Lesions in Native Kidney Biopsy Specimens: Results from the Boston Kidney Biopsy Cohort Study. J Am Soc Nephrol. 2018;29(8): 2213–2224. [PubMed: 29866798]

17. Moe SM, Pampalone AJ, Ofner S, Rosenman M, Teal E, Hui SL. Association of hepatitis C virus infection with prevalence and development of kidney disease. Am J Kidney Dis. 2008;51(6): 885–892. [PubMed: 18440680]

18. Rosenman M, He J, Martin J, et al. Database queries for hospitalizations for acute congestive heart failure: flexible methods and validation based on set theory. J Am Med Inform Assoc. 2014;21(2): 345–352. [PubMed: 24113802]

19. Zhu VJ, Tu W, Rosenman MB, Overhage JM. Nonadherence to Oral Antihyperglycemic Agents: Subsequent Hospitalization and Mortality among Patients with Type 2 Diabetes in Clinical Practice. Stud Health Technol Inform. 2015;216: 60–63. [PubMed: 26262010]

20. Levey AS, Stevens LA, Schmid CH, et al. A new equation to estimate glomerular filtration rate. Ann Intern Med. 2009;150(9): 604–612. [PubMed: 19414839]

21. Bajema IM, Wilhelmus S, Alpers CE, et al. Revision of the International Society of Nephrology/Renal Pathology Society classification for lupus nephritis: clarification of definitions, and modified National Institutes of Health activity and chronicity indices. Kidney Int. 2018;93(4): 789–796. [PubMed: 29459092]

22. Stout LC, Kumar S, Whorton EB. Focal mesangiolysis and the pathogenesis of the Kimmelstiel-Wilson nodule. Hum Pathol. 1993;24(1): 77–89. [PubMed: 8418016]

23. Lusco MA, Fogo AB, Najafian B, Alpers CE. AJKD Atlas of Renal Pathology: Idiopathic Nodular Sclerosis. Am J Kidney Dis. 2016;68(4): e19–e20. [PubMed: 27664479]

24. Moons KG, Kengne AP, Woodward M, et al. Risk prediction models: I. Development, internal validation, and assessing the incremental value of a new (bio)marker. Heart. 2012;98(9): 683–690. [PubMed: 22397945]

25. Farrington CP. Residuals for proportional hazards models with interval-censored survival data. Biometrics. 2000;56(2): 473–482. [PubMed: 10877306]

26. Tangri N, Grams ME, Levey AS, et al. Multinational Assessment of Accuracy of Equations for Predicting Risk of Kidney Failure: A Meta-analysis. Jama. 2016;315(2): 164–174. [PubMed: 26757465]

27. Sethi S, Haas M, Markowitz GS, et al. Mayo Clinic/Renal Pathology Society Consensus Report on Pathologic Classification, Diagnosis, and Reporting of GN. J Am Soc Nephrol. 2016;27(5): 1278–1287. [PubMed: 26567243]

28. Striker GE, Schainuck LI, Cutler RE, Benditt EP. Structural-functional correlations in renal disease. I. A method for assaying and classifying histopathologic changes in renal disease. Hum Pathol. 1970;1(4): 615–630. [PubMed: 5521735]

29. Schainuck LI, Striker GE, Cutler RE, Benditt EP. Structural-functional correlations in renal disease. II. The correlations. Hum Pathol. 1970;1(4): 631–641. [PubMed: 5521736]

30. Cameron JS, Hicks J. The introduction of renal biopsy into nephrology from 1901 to 1961: a paradigm of the forming of nephrology by technology. Am J Nephrol. 1997;17(3–4): 347–358. [PubMed: 9189255]

31. Ju W, Nair V, Smith S, et al. Tissue transcriptome-driven identification of epidermal growth factor as a chronic kidney disease biomarker. Sci Transl Med. 2015;7(316): 316ra193.

32. Winfree S, Ferkowicz MJ, Dagher PC, et al. Large-scale 3-dimensional quantitative imaging of tissues: state-of-the-art and translational implications. Transl Res. 2017;189: 1–12. [PubMed: 28784428]

33. Winfree S, Khan S, Micanovic R, et al. Quantitative Three-Dimensional Tissue Cytometry to Study Kidney Tissue and Resident Immune Cells. J Am Soc Nephrol. 2017;28(7): 2108–2118. [PubMed: 28154201]

34. Huang S, Sheng X, Susztak K. The kidney transcriptome, from single cells to whole organs and back. Curr Opin Nephrol Hypertens. 2019;28(3): 219–226. [PubMed: 30844884]

35. Woroniecka KI, Park AS, Mohtat D, Thomas DB, Pullman JM, Susztak K. Transcriptome analysis of human diabetic kidney disease. Diabetes. 2011;60(9): 2354–2369. [PubMed: 21752957]

36. Gillies CE, Putler R, Menon R, et al. An eQTL Landscape of Kidney Tissue in Human Nephrotic Syndrome. Am J Hum Genet. 2018;103(2): 232–244. [PubMed: 30057032]
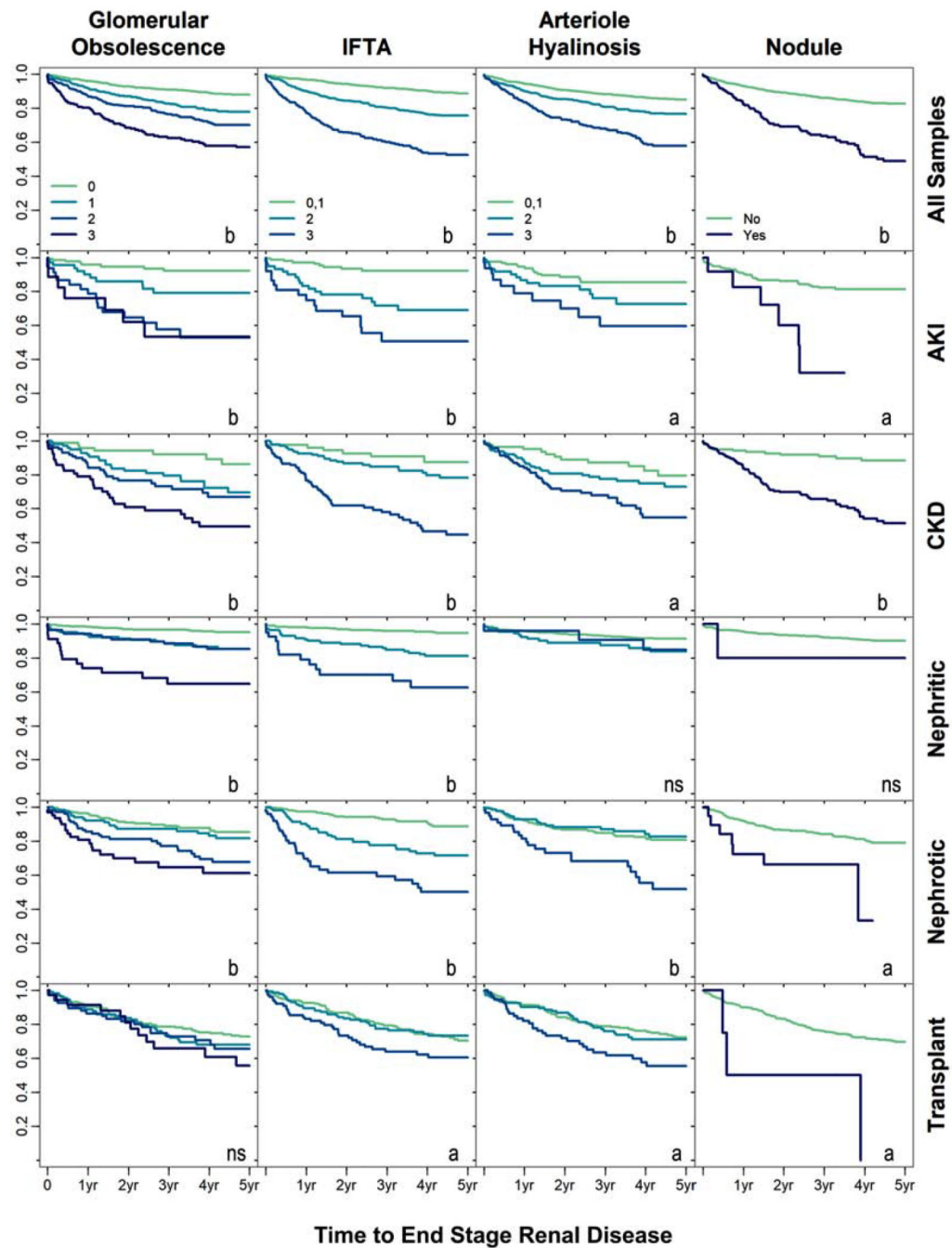
Figure 1:

Kaplan-Meier curves are depicted for the relationship between five histopathologic variables with incident ESRD across the entire cohort (row 1) and in sub-group analyses (rows 2–6). All curves are depicted as unadjusted. Unadjusted significance at P < 0.05 is acknowledged by "*a*" and significance at P < 0.001 by "*b*". For glomerular obsolescence, comparisons were made to samples with 10% obsolescence (0). For interstitial fibrosis and tubular atrophy (IFTA) and hyaline arteriolosclerosis, comparisons were made to the combined "none" and "mild" groups (0,1). Sub-groups were categorized based on their primary pathologic

diagnosis as assigned by a pathologist. AKI – acute kidney injury, CKD – chronic kidney disease, nephritic – nephritic syndrome, nephrotic – nephrotic syndrome, transplant – transplant-related diagnosis.

Table 1:

Demographics, co-morbidities, baseline clinical characteristics of the Biopsy Biobank Cohort of Indiana

Characteristic	Value
Age at biopsy	43 (18–58)
Female sex (%)	1351 (49.7)
Race:	
African-American (%)	681 (25.0)
Caucasian (%)	1954 (71.8)
Other (%)	85 (3.1)
Hispanic Ethnicity (%)	26 (1.0)
Weight (kg)	82.6 (68.0–98.9)
Co-morbidities:	
Congestive heart failure (%)	796 (29.3)
Peripheral vascular disease (%)	337 (12.4)
Diabetes mellitus (%)	1029 (37.8)
Hypertension (%)	1069 (39.3)
Coronary artery disease (%)	803 (29.5)
Smoking history, current or prior	1084 (39.9)
Peak proteinuria +/− 90 d of index (g/d)[b]	2.1 (0.6–5.9)
eGFR at biopsy (ml/min/1.73 m^2)	38.7 (20.4–60.5)
Duration of follow-up, days	1145 (354–1825)
Histopathologic features:	
Glomerular obsolescence	10% (0%–31.5%)
Interstitial fibrosis / tubular atrophy	
Severe	393 (14.4)
Moderate	737 (27.1)
Mild	1590 (58.5)
Arteriolar hyalinosis	
Severe	314 (11.5)
Moderate	638 (23.5)
Mild	595 (21.9)
Nodular mesangial sclerosis present	257 (9.4)
Crescent present	379 (13.9)

Values for categorical varialbes given as median [interquartile range]; values for categorical variables given as count (percentage of total).

[a]Proteinuria as measured by either urine protein-creatinine ratio or 24 h urine protein collection.

Table 2:

Primary diagnoses and groups of individuals in the Biopsy Biobank Cohort of Indiana

Diagnosis (Group)	No. (%)	
Acute kidney injury	281 (10.3%)	
- Acute interstitial nephritis	4.4%	120
- Acute tubular necrosis	2.8%	75
- Cholesterol emboli	0.3%	9
- Thrombotic microangiopathy	2.6%	72
Chronic kidney disease	12.9%	352
- Chronic tubulointerstitial nephritis	0.6%	16
- Diabetic nephropathy	8.8%	238
- Diffuse global glomerulosclerosis	0.4%	10
- Hypertensive nephropathy	2.6%	71
- Idiopathic nodular glomerulosclerosis	0.3%	7
Nephritic syndrome	29.7%	809
- Anti-GBM	0.1%	3
- ANCA-disease	2.7%	74
- C1Q nephropathy	0.0%	1
- C3 glomerulopathy	1.1%	29
- IGA nephropathy	11.8%	320
- IGM nephropathy	0.3%	7
- Lupus nephritis	8.7%	237
- Membranoproliferative glomerulonephritis	2.2%	60
- Post-infectious glomerulonephritis	1.0%	26
- Proliferative glomerulonephritis, not otherwise specified	2.0%	55
Nephrotic syndrome	21.0%	571
- Focal segmental glomerulosclerosis	9.1%	247
- HIVAN	0.1%	3
- Minimal change disease	3.8%	104
- Membranous nephropathy	4.8%	130
- Amyloidosis[a]	1.7%	45
- Paraprotein-associated kidney disease (non-amyloid)[a]	1.5%	42
Kidney Transplant	18.4%	500
- Acute cellular rejection	13.6%	370
- Antibody mediated rejection	0.7%	18
- BK nephropathy	0.8%	22
- Chronic allograft rejection	2.4%	64
- Chronic transplant glomerulopathy	0.9%	25
- Harvest-related ischemia	0.0%	1

Diagnosis (Group)	No. (%)	
Other	7.6%	207
- Structural or infectious disease	0.4%	12
- Fabry disease	0.2%	5
- Granulomatous interstitial nephritis or sickle cell nephropathy	0.2%	5
- Normal or non-diagnostic	4.9%	133
- Thin basement membrane	2.4%	64

[a]The primary diagnosis of amyloidosis includes AA and AL amyloidosis. The primary diagnosis of paraprotein-associated kidney disease (non-amyloid) includes all paraprotein diagnoses without amyloid deposition, including, but not limited to myeloma cast nephropathy, light chain deposition disease, proliferative glomerulonephritis with monoclonal immunoglobulin deposits, and Waldenström's macroglobulinemia.

Table 3:

Univariable and multivariable analysis of clinical exposure variables for hazard of kidney failure in individuals in the Biopsy Biobank Cohort of Indiana

Variable	Univariable Analysis[b]			Adj Clinical Model[c]		
	HR (95% CI)	r^2	C	Adj HR (95% CI)	r^2	C
Variable						
Age, per 1-year older	1.01 (1.01–1.02)[a]	0.93%	0.57	0.98 (0.97–0.99)[a]		
African American race [*]	1.80 (1.48–2.20)[a]	1.22%	0.56	1.88 (1.53–2.31)[a]		
Male sex	1.09 (0.90–1.32)	0.03%	0.51	0.97 (0.79–1.18)		
CHF	2.87 (2.36–3.48)[a]	4.00%	0.62	1.34 (1.07–1.68)[a]		
PVD	2.47 (1.98–3.09)[a]	1.95%	0.56	1.34 (1.05–1.70)[a]		
Diabetes	2.12 (1.75–2.58)[a]	2.10%	0.59	1.16 (0.93–1.46)		
Hypertension	1.97 (1.62–2.40)[a]	1.71%	0.58	1.26 (1.01–1.56)[a]		
CAD	2.60 (2.14–3.15)[a]	3.28%	0.61	1.36 (1.07–1.72)[a]		
Smoking history, current or prior	2.02 (1.66–2.45)[a]	1.83%	0.59	1.24 (1.00–1.54)[a]		
Proteinuria	1.05 (1.03–1.06)[a]	1.85%	0.65	1.04 (1.03–1.05)[a]		
Baseline eGFR (per 10 ml/min/1.73m^2 greater)	0.69 (0.66–0.73)[a]	12.85%	0.81	0.85 (0.80–0.92)[a,d]		
Fully Adjusted model					32.0%	0.912

Based on 411 individuals with the kidney failure outcome (15.1% of total).

[a] Significant comparison with $p < 0.05$.

[b] Unadjusted hazard ratios by Cox proportional hazard test.

[c] The adjusted clinical model by Cox regression model.

[d] Both the baseline eGFR and time interaction term (eGFR x time) per 365 days were included in the adjusted model.

[*] reference group: _____.

CI – confidence interval, CHF – congestive heart failure, PVD – peripheral vascular disease, CAD – coronary artery disease, Adj – adjusted; C, C-statistic

Table 4:

Univariable and multivariable analysis of clinical and histopathologic variables for hazard of kidney failure in individuals in the Biopsy Biobank Cohort of Indiana

	Univariable Analysis[b]		Clinical-Pathology Model[c]			
	HR (95% CI)	r²	Adj. HR (95% CI)	r²	C	NRI
Variable						
Arteriolar Hyalinosis		3.15%		32.24%	0.694	3.2%[d]
Moderate	1.68 (1.33–2.12)[a]		1.14 (0.87–1.49)			
Severe	3.30 (2.60–4.19)[a]		1.53 (1.14–2.05)[a]			
IFTA		7.31%		32.67%	0.705	4.6%[d]
Moderate	2.48 (1.95–3.16)[a]		1.52 (1.17–1.98)[a]			
Severe	5.92 (4.66–7.52)[a]		1.99 (1.52–2.59)[a]			
Crescent	0.71 (0.51–0.97)[a]	0.18%	0.81 (0.58–1.13)	32.07%	0.693	1.1%
Nodule	3.24 (2.55–4.10)[a]	2.71%	1.18 (0.89–1.56)	32.06%	0.694	1.0%
Glomerular Obsolescence [*]		4.65%		32.67%	0.702	2.9%[d]
11%–30%	1.97 (1.51–2.57)[a]		1.33 (1.01–1.77)[a]			
31%–60%	2.83 (2.18–3.67)[a]		1.75 (1.31–2.33)[a]			
>60%	4.79 (3.62–6.34)[a]		2.03 (1.51–2.74)[a]			
Full model				33.01%	0.915	5.1%[d]

Based on 411 individuals with the kidney failure outcome (15.1% of total).

[a] Significant comparison with p < 0.05.

[b] Unadjusted hazard ratios by Cox proportional hazard test are presented.

[c] The adjusted hazard ratio is provided for each histopathologic variable by Cox regression model. Each variable was adjusted after addition to the entire adjusted clinical mode in Table 3.

[d] The net reclassification index (NRI) is significant with an adjusted p < 0.05.

[*] Reference group: 0%–10% of kidney affected.

CI – confidence interval, IFTA – interstitial fibrosis and tubular atrophy, Crescent – fibrocellular or cellular crescent present, Nodule – nodular mesangial sclerosis present, Adj – adjusted, C – C-statistic.

Table 5:

Multivariable sub-group analysis for the hazard of kidney failure in individuals in the Biopsy Biobank Cohort of Indiana

	All (N = 2513)	Diagnosis Subgroup				
		AKI (n = 281)	CKD (n = 352)	Nephritic (n = 809)	Nephrotic (n = 571)	Transplantrelated (n = 500)
No. with Outcome	401 (16.0%)	43 (15.3%)	84 (23.9%)	62 (7.7%)	92 (16.1%)	120 (24.0%)
Histopathologic Feature						
Arteriolar Hyalinosis						
Moderate	1.09 (0.83–1.43)	2.20 (1.08.4.47)[a]	1.64 (0.78–3.45)	1.21 (0.60–2.42)	0.75 (0.39–1.44)	0.99 (0.61–1.61)
Severe[b]	1.51 (1.13.2.02)[a]	2.62 (1.18.5.83)[a]	2.02 (1.23.5.60)[a]	1.06 (0.30–3.78)	1.39 (0.70–2.76)	1.49 (0.87–2.57)
IFTA						
Moderate[c]	1.49 (1.14.1.95)[a]	6.10 (2.69.13.81)[a]	1.35 (0.55–3.30)	3.33 (1.72.6.44)[a]	1.41 (0.77–2.59)	0.55 (0.35–0.87)[a]
Severe[c]	1.93 (1.47.2.52)[a]	6.49 (2.84.14.82)[a]	1.98 (0.85–4.57)	3.09 (1.46.6.54)[a]	1.60 (0.84–3.04)	0.98 (0.61–1.54)
Crescent	0.83 (0.59–1.16)	0.62 (0.15–2.60)	2.73 (0.34.21.78)	0.95 (0.54–1.65)	0.86 (0.20–3.71)	1.50 (0.42–5.38)
Nodule	1.15 (0.86–1.52)	2.54 (1.04.6.18)[a]	1.79 (0.81–3.95)	0.87 (0.12–6.65)	1.40 (0.61–3.21)	2.01 (0.61–6.68)
Glomerular Obsolescence[*]						
11–30%	1.26 (0.95–1.67)	3.06 (1.22.7.69)[a]	1.65 (0.67–4.01)	2.03 (0.97–4.23)	1.14 (0.60–2.13)	0.96 (0.59–1.54)
31–60%[c]	1.67 (1.25.2.23)[a]	9.07 (3.83.21.48)[a]	1.76 (0.73–4.24)	2.83 (1.28.6.23)[a]	1.37 (0.73–2.58)	1.13 (0.63–2.04)
>60%[c]	1.91 (1.42.2.58)[a]	7.90 (2.80.22.28)[a]	2.98 (1.22.7.28)[a]	2.84 (1.28.6.28)[a]	1.42 (0.73–2.74)	0.93 (0.48–1.84)

Values are given as adjusted hazard ratio (95% confidence interval).

[a] Significant comparison with p < 0.05. The adjusted hazard ratio is provided for each histopathologic variable by Cox regression model. A single model including all demographic and clinical variables, as well as primary diagnosis sub-group and diagnosis interaction terms was fitted for each histopathologic covariate.

[b,c] Heterogeneity is present for this histopathologic characteristic across the sub-groups with: (b) p < 0.05 or (c) p < 0.001 for the interaction term between the histopathologic feature and sub-group.

[*] Reference group: 0%–10% of kidney affected.

IFTA – interstitial fibrosis and tubular atrophy, Crescent – fibrocellular or cellular crescent present, Nodule – nodular mesangial sclerosis present, AKI – acute kidney injury, CKD – chronic kidney disease.